C(sp³)–H Carboxylation via Carbene/Photoredox Cooperative Catalysis

Cullen R. Schull, Jing Cao, Sophia R. Mitton-Fry, Mara Mrksich and Karl A. Scheidt*

C(sp³)–H bond functionalization is a powerful strategy for the synthesis of organic compounds due their abundance in simple starting materials. Photoredox catalysis has led to a diverse array of enabling C(sp³)–H activation strategies; however, the direct functionalization of C(sp³)–H to carboxylic acid derivatives remains underexplored. Disclosed herein is the development of a cooperative NHC/photoredox-catalyzed C(sp³)–H esterification transformation. This method enables access to benzylic, α–heteroatom, and formal β-esterification products in good to excellent yields under mild reaction conditions.

Introduction

Carboxylic acids and their derivatives (e.g., esters, amides) are ubiquitous in biology, playing important roles in facilitating protein synthesis,[1] regulating lipid homeostasis,[2] and mediating cellular signaling pathways.[3] Beyond natural systems, these related functional groups are valuable synthetic handles[4] and as such, have demonstrated utility in pharmaceuticals,[5] polymers,[6] and agrochemicals (Figure 1A).[7] With such widespread applications, the selective incorporation of carboxyl moieties from activated C–H bonds offers a promising, streamlined strategy to access these valuable carbonyl-containing groups. Despite the tremendous advancements in C–H functionalization,[8] the direct C(sp³)–H carboxylation remains a challenging transformation.

The recent resurgence of photochemistry has driven the discovery of new bond disconnections not accessible through traditional two-electron pathways.[9] In particular, the development of photochemical methodologies utilizing C1 sources (e.g., CO_2, $HCOO^-$) to readily access carboxylic acid functionalities has garnered significant attention. Contemporary photochemical radical carboxylation strategies typically operate via the challenging direct reduction of CO_2 ($E_{1/2}$ = −2.21 V vs SCE)[10] or hydrogen atom abstraction from formate salts to access a highly reactive $CO_2^{•-}$ intermediate. The nascent $CO_2^{•-}$ is well-documented for its reactivity in undergoing radical addition into activated and unactivated alkenes exemplified by the elegant work of Wickens,[11] Yu,[12] and others (Figure 1B).[13] Similarly, the closely related alkoxycarbonyl radical has been accessed through a variety of activation methods including single-electron activation of radical precursors,[14] triplet energy transfer to oximes,[15] and hydrogen atom abstraction of alkyl formates[16] for radical esterification. However, these strategies rely
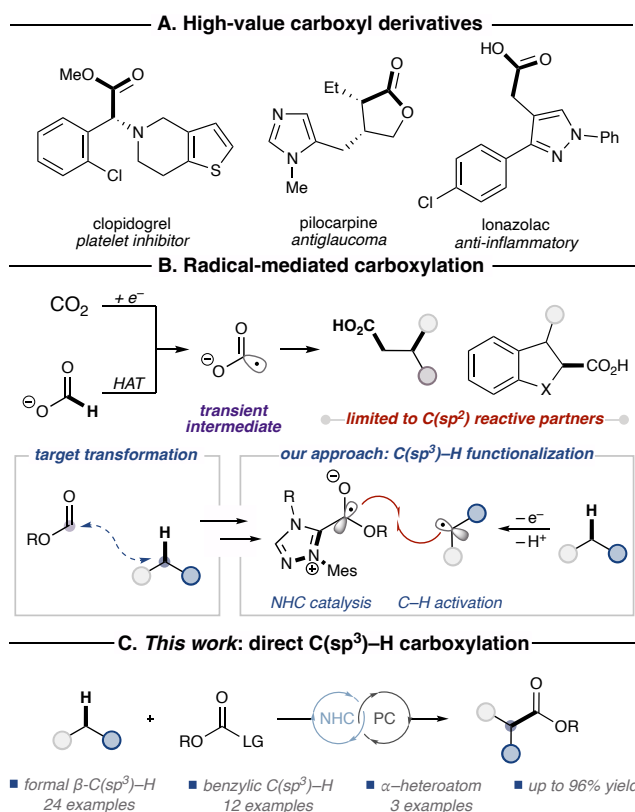

Figure 1. (A) Examples of valuable carboxyl derivatives; (B) Radical-mediated carboxylation strategies and our design; (C) Dual NHC/photoredox C(sp³)–H esterification.

on transient carboxyl radical intermediates limiting their reactivity to sp²-hybridized systems (e.g., radical acceptors). In comparison, the *direct* carboxylation of C(sp³)–H coupling partners is rather underdeveloped.

In 2015, the Murakami group disclosed an ortho-directed benzylic C(sp³)–H carboxylation proceeding through an *o*-quinodimethane intermediate.[17] Later, they developed a copper-catalyzed allylic C(sp³)–H carboxylation,[18] and a nickel-catalyzed benzylic and aliphatic carboxylation.[19] In 2017, the Jamison group developed an α–amino carboxylation process operating through the challenging reduction of carbon dioxide.[20] Despite the utility of these strategies, they are reliant on activation by UV irradiation, often require a metal catalyst, and in some instances, need significant substrate loading to mediate the process. To address these

limitations, the König group developed the first visible-light mediated C(sp3)–H benzylic carboxylation by a photoredox-thiol manifold to access a carbanion for carboxylation with CO2.[21] While this strategy is enabling, it generates a highly reactive carbanion intermediate thereby potentially limiting its utility in complex molecule synthesis. Consequently, the development of a milder radical cross-coupling process would provide access to broader substrate classes and corresponding products.

Over the past five years, our group along with the groups of Ohmiya, Studer, Chi, and others have focused on the development of NHC-catalyzed radical reactions to form carbon-carbon bonds.[22] In 2019, the Ohmiya group was the first to achieve efficient radical cross-coupling through a single-electron oxidation of the Breslow intermediate with redox-active esters to afford ketone products.[23] Shortly thereafter, our group[24] and Studer's group[25] independently accessed azolium-ketyl radicals *via* photocatalytic single-electron reduction to access ketones and β-trifluoromethylketones, respectively. Following these reports, NHC-stabilized ketyl radicals have been leveraged in various two-component and three-component manifolds to access diverse ketone products. In contrast, the development of NHC-stabilized radicals to access other carbonyl functionalities is *significantly less established*. Recently, our group was the first to explore azolium-stabilized alkoxycarbonyl radicals to afford challenging carboxylated products.[26] However, the laborious pre-functionalization of benzylic radical sources (e.g., potassium trifluoroborate salts) and stoichiometric azolium esters were required to enable the photocatalyzed two-component radical cross-coupling. In contrast, there are limited reports of an organocatalytic radical cross-coupling of alkoxycarbonyl radicals with carbon-centered radicals derived from C(sp3)–H bonds.

Building on the developing area of carbene-stabilized single electron species, we questioned whether NHC-stabilized alkoxycarbonyl radicals generated *in situ* could enable the direct carboxylation of simple C(sp3)–H bonds previously inaccessible with transient carboxyl radical intermediates (*vide supra*). Inspired by recent work in photoredox C–H activation,[8b] we sought to develop a selective carboxylation directed by inherent redox properties of specific functional groups. In our proposed reaction design, we hypothesized that a variety of electron-rich substrates could undergo single-electron oxidation by a photocatalyst and subsequent deprotonation by a mild base to access carbon-centered radicals. In a connected process, the NHC catalyst can be carboxylated *in situ* with pyrocarbonate and undergo a single-electron reduction thereby closing the photocatalytic cycle. The ensuing NHC-stabilized alkoxycarbonyl radical could undergo selective radical cross-coupling with transient carbon-centered radical partners to afford carboxylated products.

Results and discussion

We commenced our investigations of the direct carboxylation with silyl enol ether (**1a**) as our model electron-rich substrate and diethyl pyrocarbonate (**2a**) as our carboxyl source. Due to the high oxidation potential of **1a** (+1.52 V vs. SCE, See SI for CV experiments) along with various silyl enol ethers, a strongly oxidizing photocatalyst was imperative for reaction success. As a result, we initially surveyed 3CzClIPN (*$E_{1/2}^{red}$ = +1.56 V vs. SCE),[27] for its high excited state oxidation potential to effectively generate the silyl enol ether radical cation intermediate. Additionally, **NHC-1** was selected as the initial

NHC catalyst due to its previous reactivity in NHC radical catalysis.[28] To our surprise, these initial reaction conditions provided the desired product in 65% yield by ^{1}H NMR spectroscopy (Table 1, Entry 1). Notably, no α-carboxylation was detected, and we suspect this is due to a polarity mismatch as only highly electrophilic radicals (e.g. trifluoromethyl & trifluoromethoxyl radicals)[29] have demonstrated reactivity with silyl enol ethers. Additionally, no double addition products were observed. We hypothesize this is due to an increase in oxidation potential in the product, thereby preventing a second oxidation. Subsequent photocatalyst screening with other highly oxidizing organophotocatalysts 4CzIPN (*$E_{1/2}^{red}$ = +1.43 V vs. SCE) and 5CzBn ($E_{1/2}$ = +1.41 V vs. SCE)[27] resulted in diminished product formation likely due to a slow oxidation of **1a** (Table 1, Entries 2-3). Switching the reaction solvent from acetonitrile to dichloroethane resulted in diminished reactivity and unreacted starting material (Table 1, Entry 4).

Table 1. Optimization of Reaction Conditions
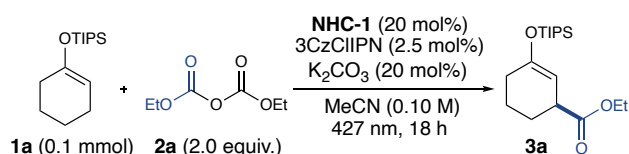
entry	deviation from standard	Yield (%)[a]
1	none	65[b]
2	**4CzIPN** instead of **3CzClIPN**	38
3	**5CzBN** instead of **3CzClIPN**	38
4	DCE instead of MeCN	23
5	Cs2CO3 instead of K2CO3	47
6	1,3,5-collidine instead of K2CO3	0
7	x equiv. **2a** (1.0, 2.0, 3.0)	43, 65[b], 63
8	x mol% K2CO3 (20, 40, 60)	65[b], 77, 72
9	**NHC-2** instead of **NHC-1**	79
10	**NHC-3** instead of **NHC-1**	0
11	**NHC-4** instead of **NHC-1**	0
12	**NHC-2**, 40 mol% K2CO3	89
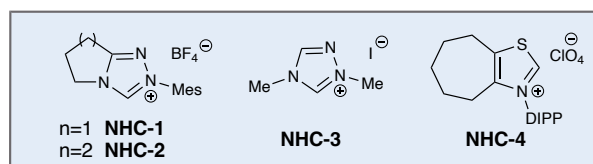
[a] ^{1}H NMR yield of crude mixture with 1,3,5-trimethoxybenzene as a standard. [b] Average yield over three experiments.

Substituting K2CO3 with Cs2CO3 provided a decreased yield, and replacement with an organic base resulted in no product formation (Table 1, Entries 5-6). Investigating the loading of diethyl pyrocarbonate and K2CO3 demonstrated that 40 mol% base loading with 2.0 equivalents of **2a** provided optimal product yields (Table 1, Entries 7-8). Given the proposed reaction requires both the deprotonation of the NHC and oxidized substrate **1a**, we suspect the alkoxide byproduct generated from the NHC addition into the pyrocarbonate may facilitate these deprotonation processes (Figure 4). Furthermore, the replacement of **NHC-1** with **NHC-2** resulted in a significant increase in yield (Table 1, Entry 9). In contrast, no product formation was detected when **NHC-3** and **NHC-4** were employed (Table 1, Entries 10-11). Additional increases in yield were achieved

Table 2. Formal β–Carboxylation Substrate Scope.
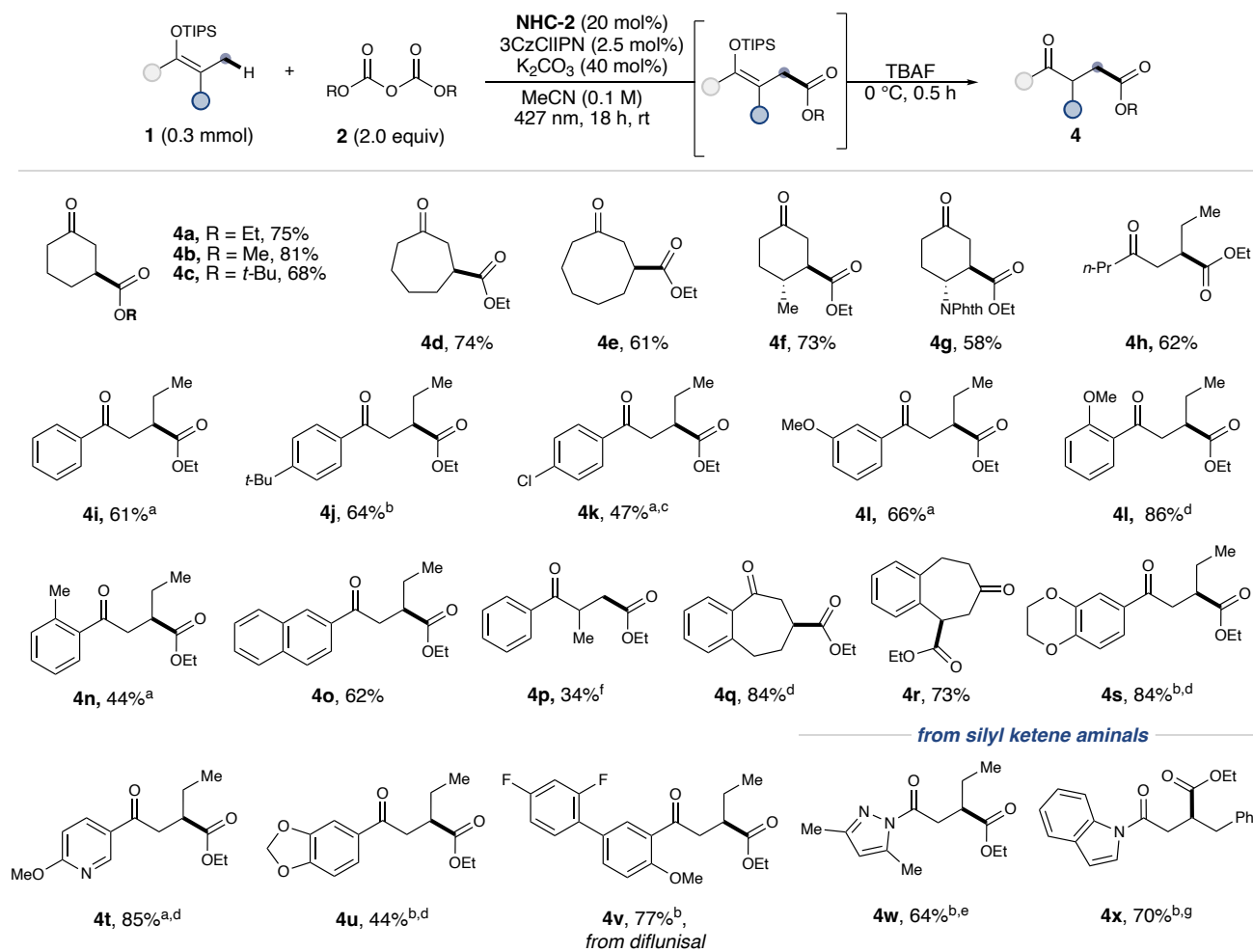
[a] 5 equiv of **2** [b] 3 equiv of **2** [c] 48 h [d] 6 h [e] 4 h [f] 3 h [g] 2 h
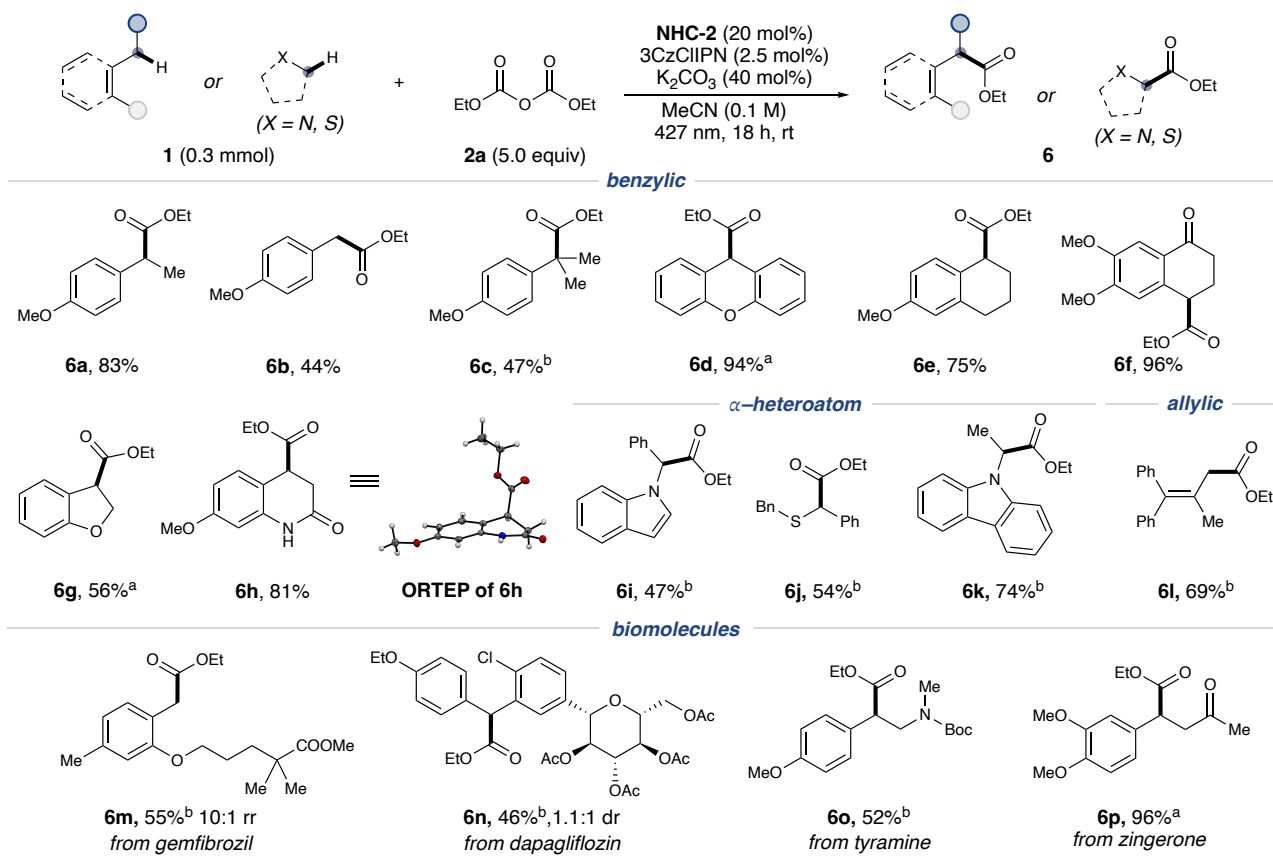
by screening **NHC-2** with optimal **NHC-1** condition (Table 1, Entry 8) providing an excellent 89% NMR yield (Table 1, Entry 12).

With optimized conditions in hand, we began evaluating the formal β-esterification substrate scope (Table 2). First, the optimized substrate **1a** was well-tolerated and isolated in high yield upon work-up to afford **4a**. The replacement of **2a** with dimethyl pyrocarbonate and di-*tert*-butyl dicarbonate afforded desired products (**4b**-**4c**) in moderate yields. Different ring sizes (**4d**-**4e**) were also tolerated in moderate to good yields. 4-Substituted cyclic silyl enol ethers afforded the esterified products **4f** and **4g** in moderate yields with the trans diastereomer as the sole product. A series of acyclic aryl-substituted silyl enol ethers were successfully employed with electron-donating or electron-withdrawing substituents, providing the corresponding products (**4h-4v**) in moderate to excellent yield. Strongly withdrawing aryl functionalities (e.g. 4-CF₃, 4-OCF₃, 3- Br) were low yielding or not productive in this methodology, likely due to a challenging initial oxidation to the radical cation due to an increase in oxidation potentials (See SI for unsuccessful substrates). On the other hand, we were delighted to discover pyridine-containing enol silane (**4t**) and silyl ketene aminals (**4w** & **4x**) were efficiently converted to formal β-esterified products, demonstrating the ability to functionalize heterocyclic-containing substrates and provide access to succinamic ester building blocks. To demonstrate

the applicability in a late-stage functionalization setting, a diflunisal (an anti-inflammatory drug) derivative was successfully transformed to the desired γ-ketoester product **4v** under our optimized conditions.

Figure 2. Scalability & Further Transformations
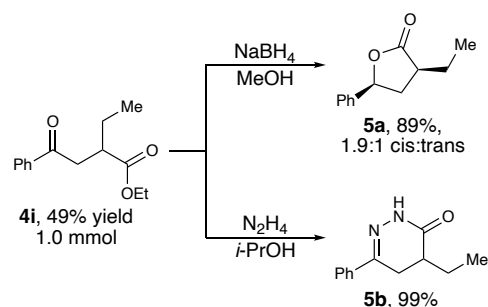
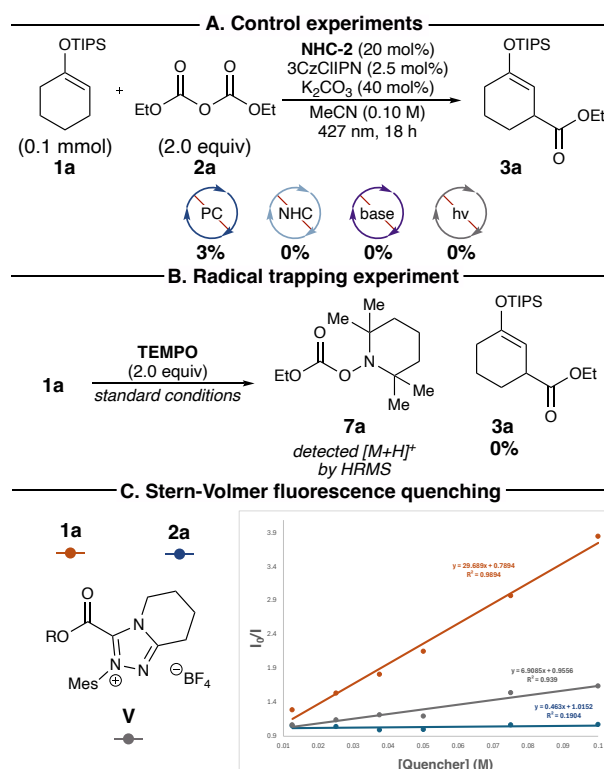To demonstrate the scalability of our reaction, silyl enol ether **1g** was efficiently converted to the desired ester **4i** in 49% yield on a 1.00 mmol scale (Figure 2). Next, we selected product **4i** to showcase the synthetic utility of γ-ketoesters. Borohydride reduction and subsequent intramolecular cyclization of **4i** provided a functionalized γ-butyrolactone derivative **5a**, a widely known structural moiety with

Table 3. Benzylic & α-Heteroatom C(sp^3)–H Substrate Scope

Reaction scheme: **1** (0.3 mmol) *or* (X = N, S) + **2a** (5.0 equiv) (EtO–CO–O–CO–OEt) → conditions: **NHC-2** (20 mol%), 3CzClIPN (2.5 mol%), K$_2$CO$_3$ (40 mol%), MeCN (0.1 M), 427 nm, 18 h, rt → **6** *or* (X = N, S)

benzylic

6a, 83%   **6b**, 44%   **6c**, 47%[b]   **6d**, 94%[a]   **6e**, 75%   **6f**, 96%

α–heteroatom   *allylic*

6g, 56%[a]   **6h**, 81%   ORTEP of 6h   **6i**, 47%[b]   **6j**, 54%[b]   **6k**, 74%[b]   **6l**, 69%[b]

biomolecules

6m, 55%[b] 10:1 rr   **6n**, 46%[b],1.1:1 dr   **6o**, 52%[b]   **6p**, 96%[a]
from gemfibrozil   *from dapagliflozin*   *from tyramine*   *from zingerone*

[a] 3 equiv of **2a** [b] 48 h

pharmaceutical activities.[30] Furthermore, treatment of **4i** with hydrazine afforded the corresponding functionalized 4,5-dihydropyrazinone **5b**, a core motif in various natural products,[31] in 99% yield.

Following the exploration and establishment of a formal β-esterification strategy, we sought to extend this method towards different substrate classes to establish broad utility to various C(sp^3)–H sources. Inspired by previous works in benzylic C(sp^3)–H functionalization,[32] our initial investigations began with 4-substituted anisole derivatives. To our delight, 4-ethylanisole furnished site-selective benzylic esterified product (**6a**) in high yields, although an increased diethyl pyrocarbonate (5.0 equiv.) loading was required to promote the full consumption of 4-ethylanisole. Furthermore, 4-methylanisole and 4-isopropylanisole were converted to the desired products (**6b & 6c**), demonstrating the ability to tolerate primary and tertiary radical intermediates, albeit in reduced yields. Other various alkoxy-substituted arenes proceeded with good efficiency (**6d-6f**). Notably, benzofuran (**6g**) and quinolone-containing (**6h**) substrates underwent the desired benzylic esterification in moderate yields. Electron-rich α-heteroatom-containing substrates were tolerated, providing access to α-amino and α-thiyl esters (**6i-6k**). A tetrasubstituted alkene was converted into the allylic esterified product in moderate yield (**6l**).

To exemplify the feasibility of our strategy in drug discovery, we pursued the late-stage benzylic functionalization of pharmaceuticals and relevant biomolecules. Gemfibrozil, a lipid-lowering drug, was functionalized with excellent regioselectivity for the ortho-benzylic position, and dapagliflozin, a drug used to treat

A. Control experiments

Scheme: (0.1 mmol) **1a** (OTIPS-cyclohexene) + (2.0 equiv) **2a** → NHC-2 (20 mol%), 3CzClIPN (2.5 mol%), K$_2$CO$_3$ (40 mol%), MeCN (0.10 M), 427 nm, 18 h → **3a**

PC 3%   NHC 0%   base 0%   hv 0%

B. Radical trapping experiment

1a → TEMPO (2.0 equiv), standard conditions → **7a** detected [M+H]$^+$ by HRMS   **3a** 0%

C. Stern-Volmer fluorescence quenching

1a   2a

Structure V: RO–C(=O)–... triazolium with Mes, BF$_4^-$

y = 29.689x + 0.7894, R^2 = 0.9894
y = 6.9085x + 0.9556, R^2 = 0.939
y = 0.463x + 1.0152, R^2 = 0.1904

I$_0$/I vs [Quencher] (M)

Figure 3. (A) Control reactions for C(sp^3)–H carboxylation; (B) Radical trapping experiment; (C) Stern-Volmer quenching experiment.

type 2 diabetes, was functionalized with benzylic site-selectivity in 46% yield (**6m & 6n**). Next, a tyramine derivative was efficiently converted in 52% yield to provide **6o**, and zingerone, a naturally derived antioxidant found in ginger, provided the desired ester **6p** in an excellent 96% yield.

After establishing this dual catalytic process, we turned our attention towards gaining a mechanistic understanding. Our initial control experiments omitting photocatalyst, NHC, base, or light resulted in trace to no product formation, thereby supporting the necessity for each of these reaction components for the desired reactivity (see SI for benzylic reaction controls). Next, a radical trapping experiment was performed with an excess of TEMPO (2.0 equiv). The expected ester TEMPO-adduct was observed via ESI-HRMS, and product formation was fully suppressed, further supporting a radical-based mechanism (Figure 3B). Stern-Volmer fluorescence quenching experiments revealed silyl enol ether (**1a**) quenches the photocatalyst at a much higher rate than the azolium ester (**V**), suggesting the photocatalytic cycle operates through a reductive quenching pathway (Figure 3C). However, the azolium ester (**V**) did demonstrate photocatalyst quenching; therefore, we cannot rule out the possibility of an oxidative quenching as an operative photocatalytic pathway.
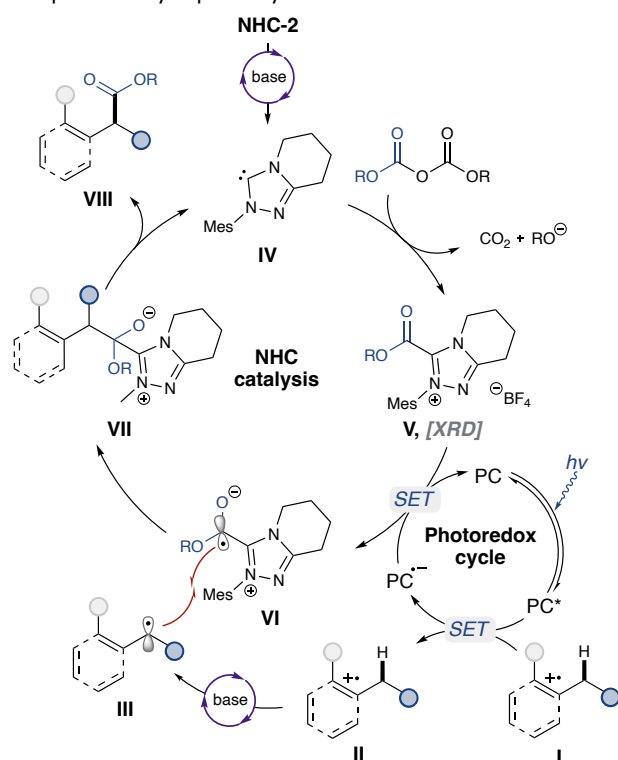

Figure 4. Proposed mechanism for the C(sp^3)–H carboxylation.

With the results of our mechanistic studies, our proposed mechanism is illustrated in Figure 4 using a generic C(sp^3)–H (**I**) as our substrate and a generic pyrocarbonate. The photocatalytic cycle commences with a single-electron oxidation of an oxidizable C(sp^3)–H substrate (**I**) to form the radical cation intermediate (**II**), which upon deprotonation generates the carbon-centered radical coupling partner (**III**). The NHC catalytic cycle begins with deprotonation of **NHC-2**, generating the reactive carbene intermediate (**IV**). Nucleophilic addition to a pyrocarbonate affords the azolium ester intermediate (**V**). Single-electron reduction of **V** closes the photocatalytic cycle and affords the NHC-alkoxycarbonyl radical intermediate (**VI**). Cross-coupling between **VI** and **III** results in a

tetrahedral intermediate **VII**. The fragmentation of **VII** closes the NHC catalytic cycle to afford the desired ester product (**VIII**).

Conclusions

In summary, we have developed a dual NHC/photoredox approach for the direct esterification of various C(sp^3)–H bonds. A broad range of active C–H bonds including β-keto, benzylic, and α-heteroatom C(sp^3)–H bonds were amenable reaction partners, enabling rapid access to synthetically useful carbonyl-containing compounds with a high degree of structural variability. In comparison to other contemporary radical carboxylation methodologies, the NHC-stabilized alkoxycarbonyl radical approach demonstrates complementary reactivity by facilitating a metal-free radical cross-coupling process and extending radical carboxylation methodologies to sp^3-hybridized coupling partners. The exploration of an enantioselective version, and the incorporation of this strategy towards complex molecule synthesis is currently underway.

Data availability

All experimental data, and detailed experimental procedures are available in the published article and ESI.†

Author Contributions

The work was conceptualized by C. R. S and K. A. S. The experiments were performed by C. R. S., J. C., S. R. M. F., and M. M. The manuscript was written through contributions of all authors. K. A. S. secured funding and supervised the entire work.

Conflicts of interest

There are no conflicts to declare.

Acknowledgements

Notes and references

1. M. V. Rodnina and W. Wintermeyer, *Curr. Opin. Struct. Biol.*, 2003, **13**, 334-340.
2. J. Luo, H. Yang and B. L. Song, *Nat. Rev. Mol. Cell Biol.*, 2020, **21**, 225-245.
3. (a) H. N. Jabbour and K. J. Sales, *Trends Endocrinol. Metab.*, 2004, **15**, 398-404; (b) I. R. Kelsall, J. Zhang, A. Knebel, J. S. C. Arthur and P. Cohen, *Proc. Natl. Acad. Sci. U.S.A.*, 2019, **116**, 13293-13298; (c) E. J. Longarini and I. Matic, *Nat. Commun.*, 2024, **15**, 4239.

4. (a) R. Takise, K. Muto and J. Yamaguchi, *Chem. Soc. Rev.*, 2017, **46**, 5864-5888; (b) L. Li, Y. Yao and N. Fu, *Eur. J. Org. Chem.*, 2023, **26**.
5. (a) L. D. Davis, *ACS Chem. Biol.*, 2008, **3**, 203-206; (b) A. Szuts and P. Szabo-Revesz, *Int. J. Pharm.*, 2012, **433**, 1-9; (c) E. M. Larsen and R. J. Johnson, *Drug Dev. Res.*, 2019, **80**, 33-47.
6. (a) A. Das and P. Theato, *Chem. Rev.*, 2016, **116**, 1434-1495; (b) J. F. R. Van Guyse, Y. Bernhard, A. Podevyn and R. Hoogenboom, *Angew. Chem., Int. Ed.*, 2023, **62**, e202303841; (c) M. Hansen-Felby, M. L. Henriksen, S. U. Pedersen and K. Daasbjerg, *Macromolecules*, 2022, **55**, 5788-5794.
7. M. J. L. Castro, C. Ojeda and A. F. Cirelli, *Environ. Chem. Lett.*, 2013, **12**, 85-95.
8. (a) H. M. Davies and D. Morton, *J. Org. Chem.*, 2016, **81**, 343-350; (b) N. Holmberg-Douglas and D. A. Nicewicz, *Chem. Rev.*, 2022, **122**, 1925-2016; (c) P. Bellotti, H. M. Huang, T. Faber and F. Glorius, *Chem. Rev.*, 2023, **123**, 4237-4352; (d) D. L. Golden, S. E. Suh and S. S. Stahl, *Nat. Rev. Chem.*, 2022, **6**, 405-427.
9. (a) M. H. Shaw, J. Twilton and D. W. MacMillan, *J. Org. Chem.*, 2016, **81**, 6898-6926; (b) D. F. Fernandez, M. Gonzalez-Esguevillas, S. Keess, F. Schafer, J. Mohr, A. Shavnya, T. Knauber, D. C. Blakemore and D. W. C. MacMillan, *Org. Lett.*, 2024, **26**, 2702-2707; (c) J. M. Smith, S. J. Harwood and P. S. Baran, *Acc. Chem. Res.*, 2018, **51**, 1807-1817; (d) N. E. S. Tay, D. Lehnherr and T. Rovis, *Chem. Rev.*, 2022, **122**, 2487-2649.
10. J. A. Rosso, S. G. Bertolotti, A. M. Braun, D. O. Mártire and M. C. Gonzalez, *J. Phys. Org. Chem.*, 2001, **14**, 300-309.
11. (a) S. N. Alektiar and Z. K. Wickens, *J. Am. Chem. Soc.*, 2021, **143**, 13022-13028; (b) M. Mikhael, S. N. Alektiar, C. S. Yeung and Z. K. Wickens, *Angew. Chem., Int. Ed.*, 2023, **62**, e202303264; (c) S. N. Alektiar, J. Han, Y. Dang, C. Z. Rubel and Z. K. Wickens, *J. Am. Chem. Soc.*, 2023, **145**, 10991-10997.
12. (a) L. Song, W. Wang, J.-P. Yue, Y.-X. Jiang, M.-K. Wei, H.-P. Zhang, S.-S. Yan, L.-L. Liao and D.-G. Yu, *Nat. Catal.*, 2022, **5**, 832-838; (b) W. Zhang, Z. Chen, Y. X. Jiang, L. L. Liao, W. Wang, J. H. Ye and D. G. Yu, *Nat. Commun.*, 2023, **14**, 3529; (c) J. H. Ye, T. Ju, H. Huang, L. L. Liao and D. G. Yu, *Acc. Chem. Res.*, 2021, **54**, 2518-2531.
13. (a) Y. Huang, J. Hou, L.-W. Zhan, Q. Zhang, W.-Y. Tang and B.-D. Li, *ACS Catal.*, 2021, **11**, 15004-15012; (b) S. R. Mangaonkar, H. Hayashi, H. Takano, W. Kanna, S. Maeda and T. Mita, *ACS Catal.*, 2023, **13**, 2482-2488; (c) P. Xu, S. Wang, H. Xu, Y.-Q. Liu, R.-B. Li, W.-W. Liu, X.-Y. Wang, M.-L. Zou, Y. Zhou, D. Guo and X. Zhu, *ACS Catal.*, 2023, **13**, 2149-2155; (d) Z. Zhao, Y. Liu, S. Wang, S. Tang, D. Ma, Z. Zhu, C. Guo and Y. Qiu, *Angew. Chem., Int. Ed.*, 2023, **62**, e202214710; (e) M.-C. Fu, J.-X. Wang, W. Ge, F.-M. Du and Y. Fu, *Org. Chem. Front.*, 2023, **10**, 35-41.
14. (a) C. C. Nawrat, C. R. Jamison, Y. Slutskyy, D. W. C. MacMillan and L. E. Overman, *J. Am. Chem. Soc.*, 2015, **137**, 11270-11273; (b) N. A. Weires, Y. Slutskyy and L. E. Overman, *Angew. Chem., Int. Ed.*, 2019, **58**, 8561-8565; (c) Y. Slutskyy and L. E. Overman, *Org. Lett.*, 2016, **18**, 2564-2567.
15. G. Tan, M. Das, H. Keum, P. Bellotti, C. Daniliuc and F. Glorius, *Nat. Chem.*, 2022, **14**, 1174-1184.
16. B. Budai, A. Leclair, Q. Wang and J. Zhu, *Angew. Chem., Int. Ed.*, 2019, **58**, 10305-10309.
17. Y. Masuda, N. Ishida and M. Murakami, *J. Am. Chem. Soc.*, 2015, **137**, 14063-14066.
18. N. Ishida, Y. Masuda, S. Uemoto and M. Murakami, *Chem. Eur. J.*, 2016, **22**, 6524-6527.
19. N. Ishida, Y. Masuda, Y. Imamura, K. Yamazaki and M. Murakami, *J. Am. Chem. Soc.*, 2019, **141**, 19611-19615.
20. H. Seo, M. H. Katcher and T. F. Jamison, *Nat. Chem.*, 2017, **9**, 453-456.
21. Q. Y. Meng, T. E. Schirmer, A. L. Berger, K. Donabauer and B. König, *J. Am. Chem. Soc.*, 2019, **141**, 11393-11397.
22. (a) A. V. Bay and K. A. Scheidt, *Trends Chem.*, 2022, **4**, 277-290; (b) K. Liu, M. Schwenzer and A. Studer, *ACS Catal.*, 2022, **12**, 11984-11999; (c) H. Cai, X. Yang, S.-C. Ren and Y. R. Chi, *ACS Catal.*, 2024, **14**, 8270-8293; (d) L. Dai and S. Ye, *Chin. Chem. Lett.*, 2021, **32**, 660-667; (e) T. Ishii, K. Nagao and H. Ohmiya, *Chem. Sci.*, 2020, **11**, 5630-5636; (f) B. Zhang, G. Yang, D. Guo and J. Wang, *Org. Chem. Front.*, 2022, **9**, 5016-5040.
23. T. Ishii, Y. Kakeno, K. Nagao and H. Ohmiya, *J. Am. Chem. Soc.*, 2019, **141**, 3854-3858.
24. A. V. Bay, K. P. Fitzpatrick, R. C. Betori and K. A. Scheidt, *Angew. Chem., Int. Ed.*, 2020, **59**, 9143-9148.
25. Q. Y. Meng, N. Doben and A. Studer, *Angew. Chem., Int. Ed.*, 2020, **59**, 19956-19960.
26. (a) J. L. Zhu and K. A. Scheidt, *Tetrahedron*, 2021, **92**, 132288; (b) N. Tanaka, J. L. Zhu, O. L. Valencia, C. R. Schull and K. A. Scheidt, *J. Am. Chem. Soc.*, 2023, **145**, 24486-24492.
27. E. Speckmeier, T. G. Fischer and K. Zeitler, *J. Am. Chem. Soc.*, 2018, **140**, 15353-15365.
28. A. V. Bay, K. P. Fitzpatrick, G. A. Gonzalez-Montiel, A. O. Farah, P. H. Cheong and K. A. Scheidt, *Angew. Chem., Int. Ed.*, 2021, **60**, 17925-17931.
29. (a) R. Ma, Z. Deng, K. H. Wang, J. Wang, D. Huang, Y. Su, Y. Hu and X. Lv, *ACS Omega*, 2022, **7**, 14357-14362; (b) L. M. Maas, C. Fasting, P. Vossnacker, N. Limberg, P. Golz, C. Muller, S. Riedel and M. N. Hopkinson, *Angew. Chem., Int. Ed.*, 2024, **63**, e202317770.
30. J. Hur, J. Jang and J. Sim, *Int. J. Mol. Sci.*, 2021, **22**, 2769.
31. K. Matsuda, K. Arima, S. Akiyama, Y. Yamada, Y. Abe, H. Suenaga, J. Hashimoto, K. Shin-Ya, M. Nishiyama and T. Wakimoto, *J. Am. Chem. Soc.*, 2022, **144**, 12954-12960.
32. (a) Q. Y. Meng, L. Lezius and A. Studer, *Nat. Commun.*, 2021, **12**, 2068; (b) B. J. Lee, K. S. DeGlopper and T. P. Yoon, *Angew. Chem., Int. Ed.*, 2020, **59**, 197-202; (c) Z. W. Hou, D. J. Liu, P. Xiong, X. L. Lai, J. Song and H. C. Xu, *Angew. Chem., Int. Ed.*, 2021, **60**, 2943-2947; (d) L. Tanwar, J. Borgel and T. Ritter, *J. Am. Chem. Soc.*, 2019, **141**, 17983-17988.